CrossMark

SENSORY PHYSIOLOGY

The unique ion permeability profile of cochlear fibrocytes and its contribution to establishing their positive resting membrane potential

Takamasa Yoshida[1,2,3] · Fumiaki Nin[1,2] · Shingo Murakami[4,5] · Genki Ogata[1,2] ·
Satoru Uetsuka[1,2,6] · Samuel Choi[7,8] · Takashi Nakagawa[3] · Hidenori Inohara[6] ·
Shizuo Komune[3,9] · Yoshihisa Kurachi[4,5] · Hiroshi Hibino[1,2,8]

Abstract Eukaryotic cells exhibit negative resting membrane potential (RMP) owing to the high K^+ permeability of the plasma membrane and the asymmetric $[K^+]$ between the extracellular and intracellular compartments. However, cochlear fibrocytes, which comprise the basolateral surface of a multi-layer epithelial-like tissue, exhibit a RMP of +5 to +12 mV in vivo. This positive RMP is critical for the formation of an endocochlear potential (EP) of +80 mV in a K^+-rich extracellular fluid, endolymph. The epithelial-like tissue bathes fibrocytes in a regular extracellular fluid, perilymph, and apically faces the endolymph. The EP, which is essential for hearing, represents the potential difference across the tissue. Using in vivo electrophysiological approaches, we describe a potential mechanism underlying the unusual RMP of guinea pig fibrocytes. The RMP was +9.0 ± 3.7 mV when fibrocytes were exposed to an artificial control perilymph ($n = 28$ cochleae). Perilymphatic perfusion of a solution containing low $[Na^+]$ (1 mM) markedly hyperpolarized the RMP to −31.1 ± 11.2 mV ($n = 10$; $p < 0.0001$ versus the control, Tukey–Kramer test after one-way ANOVA). Accordingly, the EP decreased. Little change in RMP was observed when the cells were treated with a high $[K^+]$ of 30 mM (+10.4 ± 2.3 mV; $n = 7$; $p = 0.942$ versus the control). During the infusion of a low $[Cl^-]$ solution (2.4 mM), the RMP moderately hyperpolarized to −0.9 ± 3.4 mV ($n = 5$; $p < 0.01$ versus the control), although the membranes, if governed by Cl^- permeability, should be depolarized. These observations imply that the fibrocyte membranes are more permeable to Na^+ than K^+ and Cl^-, and this unique profile and $[Na^+]$ gradient across the membranes contribute to the positive RMP.

Keywords Endocochlear potential · Inner ear · Na^+ permeability · Resting membrane potential · Spiral ligament

✉ Hiroshi Hibino
hibinoh@med.niigata-u.ac.jp

1 Department of Molecular Physiology, Niigata University School of Medicine, 1-757 Asahimachi-dori, Chuo-ku, Niigata, Niigata 951-8510, Japan

2 Center for Transdisciplinary Research, Niigata University, Niigata, Niigata 950-2181, Japan

3 Department of Otorhinolaryngology, Graduate School of Medical Sciences, Kyushu University, Fukuoka 812-8582, Japan

4 Division of Molecular and Cellular Pharmacology, Department of Pharmacology, Osaka University, Suita, Osaka 565-0871, Japan

5 The Center for Advanced Medical Engineering and Informatics, Osaka University, Suita, Osaka 565-0871, Japan

6 Department of Otorhinolaryngology-Head and Neck Surgery, Graduate School of Medicine, Osaka University, Suita, Osaka 565-0871, Japan

7 Department of Electrical and Electronics Engineering, Niigata University, Niigata 950-2181, Niigata, Japan

8 AMED-CREST, AMED, Niigata, Japan

9 Division of Otolaryngology-Head and Neck Surgery, Yuaikai Oda Hospital, Saga 849-1392, Japan

springer

Introduction

It is well known that the resting membrane potential (RMP) of eukaryotic cells is negative under physiological conditions. Excitable cells, such as neurons, cardiac myocytes, skeletal muscle cells, and smooth muscle cells, show an RMP of −50 to −90 mV, resulting from the high K^+ permeability of the membranes [11, 15, 28]. The negative RMP induced by K^+ permeability is also seen in non-excitable cells, including astroglia and retinal Müller cells [8]. Other cell types, such as epithelial cells and cardiac fibroblasts, show a less polarized RMP, but the potential never exceeds 0 mV [20, 30]. In contrast, the mammalian cochlea contains an atypical cell type that deviates from this fundamental property of having a negative RMP. Cochlear fibrocytes possess a positive RMP.

The cochlea is filled with two different fluids—the perilymph and the endolymph (Fig. 1a). While the perilymph contains ion concentrations that are typical of extracellular solutions, the endolymph exhibits a high $[K^+]$ of 150 mM and an endocochlear potential (EP) of +80 mV [9, 39]. The EP stems from a unique electrical property of the lateral cochlear wall, the epithelial-like tissue that contains fibrocytes. Sensory hair cells lie between the two lymph fluids. Acoustic stimulation opens the hair cells' mechanoelectrical transduction (MET) channels on the apical surface, which is exposed to the endolymph. This process excites the cells by causing K^+ entry from the endolymph. The highly positive EP amplifies the K^+ influx, thereby greatly sensitizing the hair cells [3, 6].

The lateral wall, which is a complex of two tissues, the stria vascularis and the spiral ligament, consists of two functional layers (Fig. 1a, b). Strial marginal cells are the typical epithelia that expose their apical surface to the endolymph and constitute the inner layer of the lateral wall. The neighboring outer layer is composed of intermediate and basal cells in the stria vascularis and fibrocytes in the spiral ligament. These three cell types are interconnected by gap junctions and therefore form an electrochemical syncytium (Fig. 1b) [17, 35–37]. The basal cells are attached to each other by tight junctions and function as a diffusion barrier [7]. Fibrocytes and the intermediate cells, which are bordered by basal cells, provide the basolateral and apical surfaces, respectively, for the syncytium. In this arrangement, the fibrocytes are bathed in the perilymph. Collectively, the syncytium likely acts as an epithelial layer [38, 39]. Between the syncytial and marginal cell layers, there is a 15-nm extracellular space termed the intrastrial space (IS), which shows a low $[K^+]$ of ~5 mM and a highly positive potential similar to the EP (Fig. 1b) [12, 14, 33].

The EP emerges from the potential difference across the two layers of the lateral wall (Fig. 1b) [26]. Under physiological conditions, the transepithelial voltage across the syncytial layer represents the positive potential in the IS. This IS potential (ISP) is primarily responsible for the EP [14, 26, 33]. In the syncytial layer, the apical RMP stems mainly from a K^+ diffusion potential on the membranes of intermediate cells, whereas the basolateral RMP corresponds to the membrane potential of the fibrocytes (Fig. 1b) [26]. In vivo, the membranes of fibrocytes continuously show a significantly positive potential of +5 to +12 mV relative to the perilymph [1, 14, 26, 41]. If this RMP was negative, like the RMPs of neurons and glial cells, then the ISP and EP would be markedly low. Therefore, this atypical characteristic of fibrocytes is a key element for hearing.

Immunohistochemical studies have identified several transporter and channel types in fibrocytes (Fig. 1b) [9, 40, 42]. Of these, Na^+/K^+ ATPases appear to maintain high $[K^+]$ in the syncytial layer by continuous K^+ uptake from the perilymph [1, 41]. However, neither physiological nor pharmacological assays targeting the channels and transporters, including the ATPases, have revealed how cells establish the positive RMP. Because fibrocytes are tightly embedded in the extracellular matrix, it seems to be difficult to access individual cells using electrodes for patch-clamp assays, as mentioned in a previous study [16]. Therefore, in the present study, we performed in vivo electrophysiological experiments. We showed that the membranes of the fibrocytes are likely to harbor a unique ion permeability profile and this element may be involved in the maintenance of the positive RMP.

Methods

Animals and ethical statement

The experimental protocol was approved by the Animal Research Committees of Niigata University School of Medicine. Experiments were carried out under the supervision of the Committees and in accordance with the Guidelines for Animal Experiments of Niigata University and the Japanese Animal Protection and Management Law. Male Hartley guinea pigs (200–400 g; SLC Inc., Hamamatsu, Japan), whose hearing levels were confirmed by normal Preyer's reflexes, were anesthetized by intraperitoneal injection of pentobarbital sodium (64.8 mg/kg; Somnopentyl; Kyoritsu Seiyaku, Tokyo, Japan). Prior to the surgical procedures (see below), toe pinch and corneal reflexes as well as respiratory rate were used as guidelines to evaluate the depth of anesthesia. When anesthesia was not sufficient, pentobarbital sodium (5 mg/kg) was additionally provided to the animals. Next, the animals were injected intramuscularly with the muscle relaxant vecuronium bromide (4 mg/kg). The surgeries were then performed as follows. The animals underwent tracheostomy and were artificially ventilated with room air. Then, the cochleae were exposed by a ventrolateral approach to insert microelectrodes [23]. During electrophysiological measurements, the depth of anesthesia was assessed by fluctuations in the heart rate.
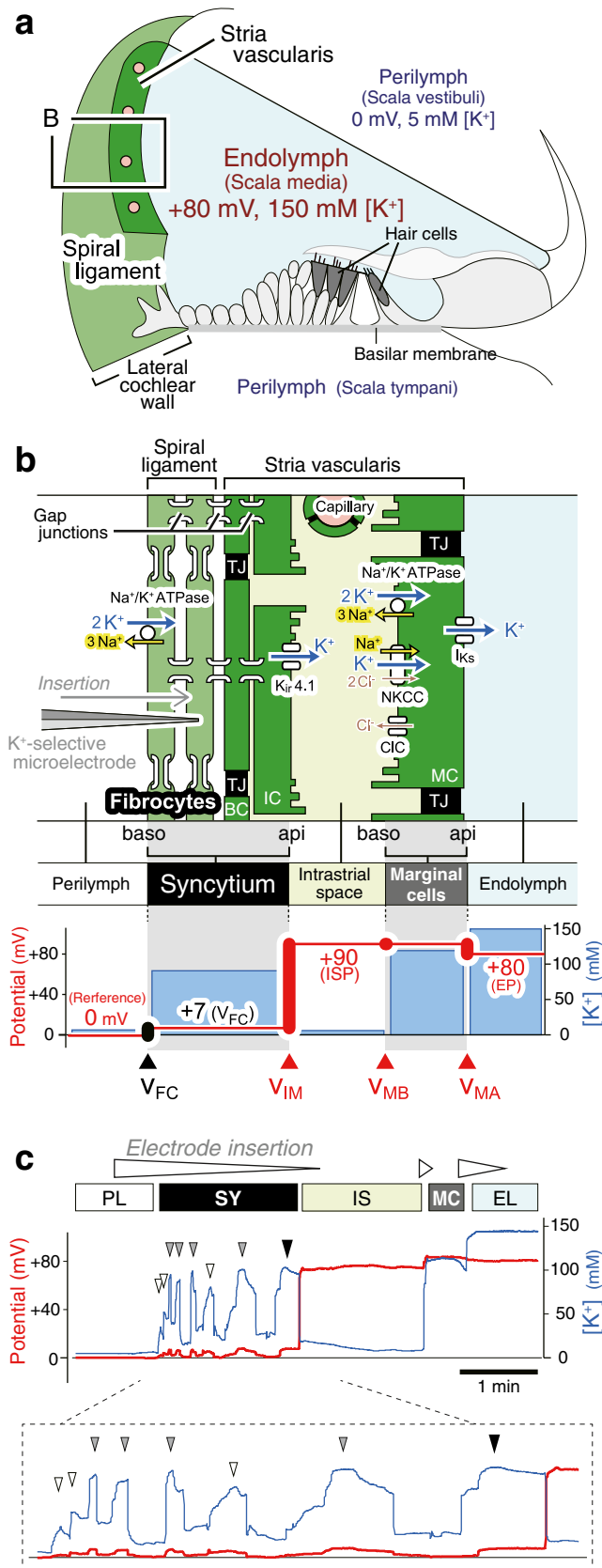
◀ **Fig. 1** Structure and electrochemical properties of the cochlea and its lateral wall. **a** Morphological characteristics of the cochlea. A cross section of the cochlea shows the three chambers: the scala vestibule, scala media, and scala tympani. The scala vestibuli and scala tympani are connected at the apex of the cochlea, providing one continuous tubule containing perilymph similar to a normal extracellular fluid. The scala media is a separate tubule filled with endolymph characterized by a high [K$^+$] of 150 mM and an endocochlear potential of +80 mV. The location of the spiral ligament and the stria vascularis, which are the constituents of the lateral wall, is also shown. **b** Cellular components of the lateral cochlear wall (*boxed region* in **a**). Fibrocytes of the ligament and the basal and intermediate cells of the stria (*BCs* and *ICs*, respectively) are all interconnected and thereby form a syncytium (*upper panel*). Fibrocytes and ICs comprise the basolateral (*baso*) and apical (*api*) surfaces in the syncytium, respectively. The location of the marginal cell (*MC*) layers, the intrastrial space (*IS*), and the channels and transporters involved in maintaining the endocochlear potential (*EP*) are described in the *upper panel*. The *lower panel* shows the potential (*red*) and [K$^+$] (*blue*) of each compartment of the lateral wall. v_{FC}, v_{IM}, v_{MB}, and v_{MA} correspond to the membrane potentials of fibrocytes, ICs, the basolateral surface of MCs, and the apical surface of MCs, respectively. *ClC*, ClC-K type Cl$^-$ channels; *ISP*, intrastrial potential; *NKCC*, Na$^+$/K$^+$/2Cl$^-$ cotransporter; *TJ*, tight junction. **c** Recording of electrochemical properties of the lateral wall. The double-barreled K$^+$ selective microelectrode, which simultaneously measured potential (*red*) and [K$^+$] (*blue*), was driven from the perilymph (*PL*) to the endolymph (*EL*) across the lateral wall (*upper panel*), as shown in the *upper panel* of **b**. In this and subsequent recordings, the wedge above the trace indicates the period during which the electrode was advanced. In the syncytial region (*SY*), *open arrowheads* point to the "spike-like" appearance of variably elevated [K$^+$] and *arrowheads filled with gray and black* show relatively "flat-topped" peaks with high [K$^+$] (see text). The compartment just prior to the intrastrial space (*IS*) (*arrowheads filled with black*) was inferred to represent the inside of this layer (see text). The measurement of the SY region is expanded in the *lower panel*. Between the IS and EL, the electrode detected the MC. **a** and **b** are modified from Fig. 1 of our previous work [26]

Anesthesia was maintained by an additional injection of pentobarbital sodium (10 mg/kg) every 1–1.5 h. Finally, the animals were sacrificed with an overdose of pentobarbital sodium (400 mg/kg) at the end of the experiments. Throughout the experiments, the body temperature of the animals was maintained at 37 °C using a heating blanket (BWT-100A, Bio Research Center, Nagoya, Japan).

Preparation of microelectrodes

Two different microelectrode types were prepared. These electrodes were fabricated from double- or single-barreled borosilicate capillary glass (WPI; Sarasota, FL, USA). For a double-barreled K$^+$-selective electrode that was subjected to measurements of [K$^+$] and potential in the lateral cochlear wall, one barrel was silanized with vaporized dimethyldichlorosilane (LS-130; Shin-Etsu, Tokyo, Japan) and filled at the tip with a liquid ion exchanger (IE190; WPI) that predominantly permeates K$^+$, and was backfilled with 150 mM KCl. The other barrel, which was non-silanized, was filled with 150 mM NaCl. Each barrel was connected via an Ag/AgCl electrode to a dual electrometer with high input-resistance (FD223a;

WPI). Calibration of each K^+-selective electrode was performed before and after the experiment using previously described methods [1, 41]. In this study, ionic concentrations were calculated based on activity coefficients for K^+ of 0.727 [22]. For the single-barreled microelectrode that was used to record the EP, the barrel was filled with 150 mM KCl and connected via an Ag/AgCl electrode to a different electrometer (MEZ-8300; Nihon Koden, Tokyo, Japan) [26].

In vivo electrophysiological recordings

Electrophysiological assays with the cochleae of live guinea pigs were performed using procedures similar to those of our previous studies [1, 26, 41]. Double-barreled K^+-selective microelectrodes and single-barreled microelectrodes, both of which were prepared as described above, were used to measure the electrochemical properties of the lateral wall and the EP, respectively. Although the values acquired by the K^+-selective electrodes represented K^+ activities, the ionic concentrations were calculated with these data using a K^+ activity coefficient of 0.727 [22] and the results are displayed in Figs. 1c, 2, 3, 4, and Supplemental Fig. 2. To insert double- and single-barreled electrodes simultaneously into the cochlea, a fenestra of roughly 200×500 μm in diameter was made on the bony wall of the second turn using a microchisel. Using an Ag/AgCl wire on the neck muscles as a reference, a K^+-selective microelectrode was inserted into the fenestra and advanced from the perilymph toward the endolymph (1–3 μm/s) using a micromanipulator (MP-285; Sutter Instrument Co., Novato, CA, USA) to record both the potential and $[K^+]$ of the lateral cochlear wall. Potentials were measured with respect to the perilymph, which was defined as 0 mV. The EP was simultaneously monitored using a single-barreled microelectrode, which was held in scala media via the above fenestra.

To perfuse solutions into the perilymphatic space, inlet and outlet holes were created on the basal cochlear turn of the scala tympani and the third turn of the scala vestibuli, respectively. Perfusates were applied at a rate of 10 μL/min using a syringe pump through a capillary tube inserted in the inlet hole as described previously [1, 41]. Although the native perilymph likely contains 130–150 mM $[Na^+]$ and ~5 mM $[K^+]$ [14, 39], for the control artificial perilymph, a solution with the following ionic composition (in mM) was used: 100 Na^+, 5 K^+, 46 N-methyl-D-glucamine (NMDG), 1.2 Ca^{2+}, 1.0 Mg^{2+}, 131.4 Cl^-, 24 HCO_3^-, 5.0 HEPES, and 4.0 glucose saturated with 5 % O_2, 5 % CO_2, and 90 % N_2 at pH 7.4 and 295 mOsm (for a justification, see below). With reference to this control solution, perfusates containing altered $[Na^+]$, $[K^+]$, or $[Cl^-]$ were prepared. For the low Na^+ (1 mM) and high K^+ (30 mM) solutions, the altered cation concentrations were compensated with equimolar NMDG (see also "Results"). Similarly, in the

low Cl^- solution (2.4 mM), Cl^- was substituted with gluconate. Notably, gluconate affects the accuracy of the K^+ exchanger in the microelectrode, to some extent [43]. Therefore, $[K^+]$ values recorded during the perfusion of the low $[Cl^-]$ solution are less quantitative; these data were used to qualitatively identify the intracellular and extracellular compartments.

In the present study, we electrophysiologically examined 110 cochleae obtained from 69 individual guinea pigs. In each cochlea, the EP was measured using a single-barreled electrode; values exceeding +70 mV were interpreted as successful measurements. Under this criterion, 84 cochleae were subjected to further experiments. In 34 cochleae, compartments within the lateral wall could not be clearly detected using a double-barreled K^+-selective microelectrode. Therefore, 50 cochleae were included in the final analysis.

References for in vivo measurements and membrane potentials

As mentioned in "In vivo electrophysiological recordings" of the Methods, in in vivo experiments, the potentials in extracellular and intracellular compartments were measured with respect to the perilymph, which was defined as 0 mV (Fig. 1b). These potentials included the EP, the ISP, and the potential inside of the syncytial layer. In the equations described in the "Results," four different membrane potentials were estimated, i.e., the potentials across fibrocyte membranes (v_{FC}), intermediate-cell membranes (v_{IM}), and the basolateral and apical surfaces of marginal cells (v_{MB} and v_{MA}, respectively) (see Fig. 1b). Note that the membranes of fibrocytes and intermediate cells correspond to the basolateral and apical surfaces of the syncytial layer, respectively. Each of these membrane potentials is expressed relative to the neighboring extracellular fluid. In other words, v_{FC} and v_{IM} represent the potentials inside the syncytial layer with respect to the perilymph and the fluid in the IS, respectively, whereas v_{MB} and v_{MA} are equivalent to the potentials inside the marginal cell with respect to the fluid in the IS and the endolymph, respectively. Importantly, the potential recorded inside the syncytial layer using an in vivo electrophysiological approach corresponded to v_{FC}.

Statistical analyses

Means ± standard deviation (SD) were used as descriptive statistics. Statistical significance was determined using a paired t test or one-way analysis of variance (ANOVA) followed by the Tukey–Kramer post-hoc test. A p value of <0.05 was considered significant. All analyses were carried out using JMP 11.0.0 (SAS Institute Japan Inc., Tokyo, Japan).
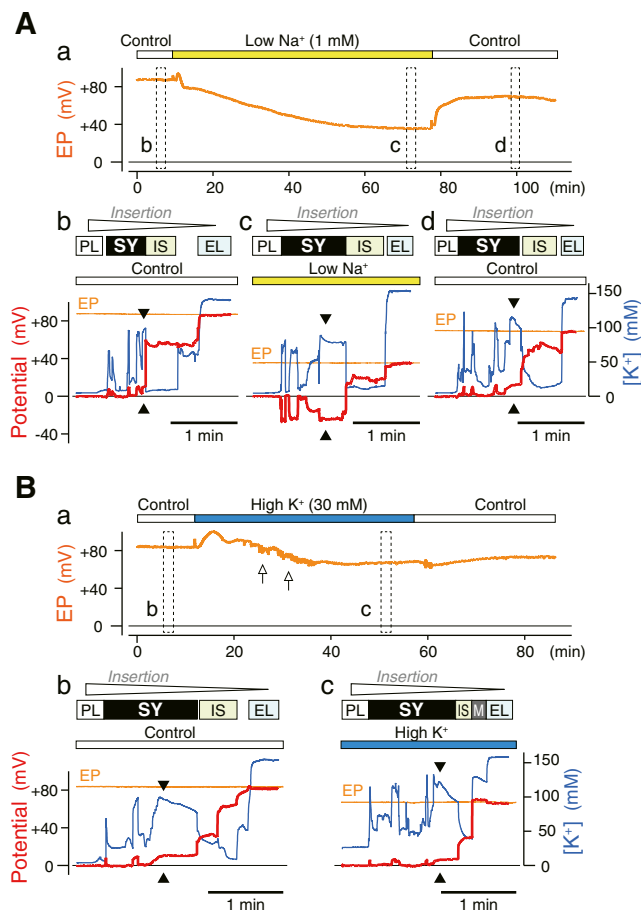
Fig. 2 Effects of varying ionic composition of the perilymph on the properties of the lateral wall. **A** Effects of the perfusion of the solution containing a low [Na$^+$] of 1 mM. In *a*, while the endocochlear potential (EP, *orange*) was monitored using a single-barreled microelectrode placed in the endolymph, different perfusates (control and low Na$^+$) were applied to the scala tympani in the period marked by the *bars* above the trace. The double-barreled microelectrodes were transiently inserted three times from the perilymph (*PL*) toward the endolymph (*EL*) during the periods marked by *boxes* in *a*. For each insertion, the potential (*red*) and [K$^+$] (*blue*) were visualized in various compartments of the lateral wall (*b*, *c*, and *d*). The traces of the EP (*orange*; see *a*) were overlaid in *b*, *c*, and *d*. Note that the compartment (*arrowheads*) just prior to the intrastrial space (*IS*) likely represents the properties inside the syncytial layer (*SY*) (see text). **B** Perfusion of a high K$^+$ solution (30 mM). Using similar procedures as those in **A**, the EP (*a*) and the electrochemical properties the lateral wall (*b* and *c*) were assayed. *Arrows* in *a* indicate flickering of the EP. In this trial, the marginal cell layer (*M*) was detected prior to the endolymph (see also Fig. 1c). *Arrowheads* point to the compartment that likely represents the properties inside the syncytial layer

Results

Identification of the profile associated with the establishment of the positive RMP in fibrocytes

To elucidate the mechanism underlying the maintenance of the positive RMP of fibrocytes, we utilized an in vivo

electrophysiological approach. The extracellular and intracellular compartments of the lateral wall can be characterized by different combinations of the potential and [K$^+$] (Fig. 1b) [14, 26, 33]. Therefore, in the assays, we used double-barreled microelectrodes sensitive to potential and [K$^+$].

Initially, we confirmed our experimental technique and the electrochemical properties of each compartment under physiological conditions by analyzing six cochleae of live guinea pigs. Figure 1c shows a representative recording of the lateral wall. A double-barreled K$^+$-selective microelectrode was inserted from the perilymph toward the endolymph across the lateral wall. Potentials were measured with respect to the perilymph (see "Methods"). The electrode in the perilymph recorded a [K$^+$] of 4.7 mM. In our earlier work [1], we attempted to hold the electrode within the fibrocytes for a few minutes to analyze the inside of the syncytial layer. However, this procedure was unsuccessful, probably because these cells contain small and highly invaginated cytoplasm [17, 35, 36]. Therefore, in this study, we continued to move the electrode forward from the perilymph to visualize the syncytial layer, as we performed previously [1, 41]. Before reaching the IS, we detected multiple compartments showing elevated [K$^+$] and potential. This result indicates that the electrode passed through several fibrocytes in the syncytial layer, consistent with previous results [1, 26, 41]. Some compartments were characterized by relatively "flat-topped" peaks with high [K$^+$] values of 89.6 to 103.4 mM and slightly positive potentials of +6.7 to +7.3 mV, demonstrating that the electrode was stably inserted into the cells constituting the syncytial layer [1]. Other compartments had a "spike-like" appearance with reduced and more variable [K$^+$] (35.5 to 80.7 mM) and potentials (+2.3 to +4.6 mV). This observation could result from processes in which the electrode penetrated the infolded processes of the fibrocytes, injured the cells, or was transiently passed through the small quantity of cytoplasm [17, 35, 36], as discussed previously [1]. When the IS was reached, the electrode recorded a low [K$^+$] of 7.8 mM and a high potential of +75.4 mV. In our previous studies, we comprehensively analyzed the syncytial region containing multiple compartments; the compartment just prior to the IS showed stable and nearly the highest values for the potential and [K$^+$] and thus likely represented the inside of the syncytial layer [1, 41]. Consistent with this observation, in the example shown in Fig. 1c, the compartment just prior to the IS exhibited the highest values within the syncytial layer (103.4 mM and +7.3 mV). This intracellular potential, which was measured with respect to the perilymph, corresponded to the membrane potential of fibrocytes (v_{FC}). On further insertion of the electrode from the IS, [K$^+$] abruptly increased to 113.8 mM (Fig. 1c), representing the inside of the marginal cell (see Fig. 1b). Finally, we recorded a [K$^+$] of 144.6 mM when advancing the electrode to the endolymph. Notably, both the IS and the endolymph show a similar potential of approximately +80 mV with respect to the perilymph, indicating little potential
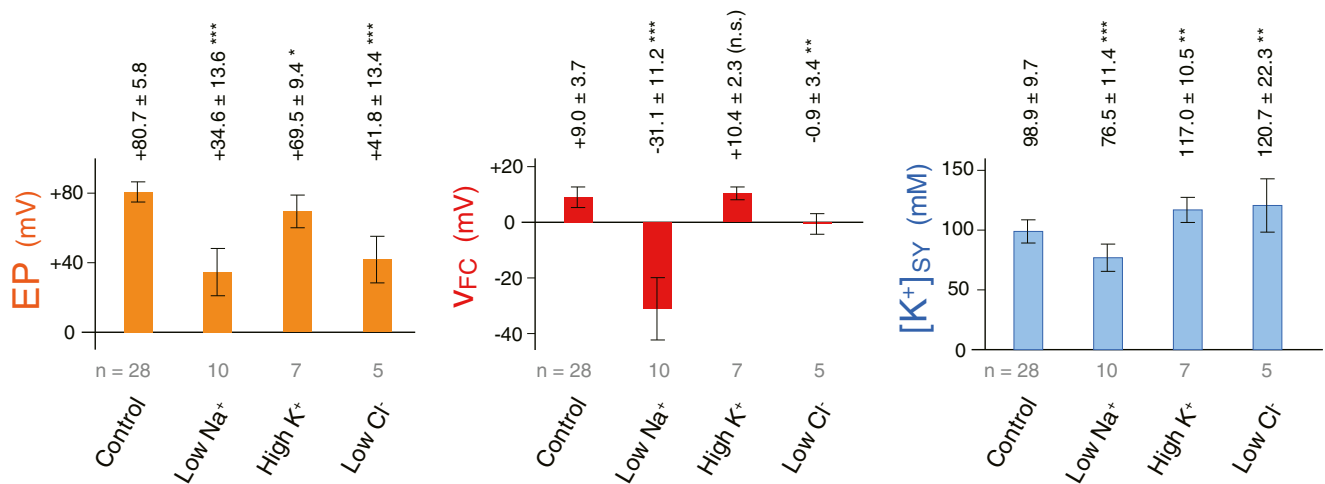
Fig. 3 Comparison of the effects of various perfusates. Displayed are means ± SD (*bars* and *error bars*, respectively) for EP values (*left panel*), syncytial potential (v_{FC}, *center panel*), and [K⁺] ([K⁺]$_{SY}$, *right panel*) during perilymphatic perfusion of four different solutions. Number of the cochleae examined is shown below the *bars*. For analyzing the EP, a minimum, stable value in each experiment was used. The syncytial data were acquired simultaneously with the EP value. The control group ($n = 28$ cochleae) included the data obtained prior to the perfusion of low Na⁺, high K⁺, and low Cl⁻ solutions ($n = 22$ cochleae as a total; see Figs. 2Ab, Bb, and Supplemental Fig. 2B) and the data obtained during the application of only artificial control perilymph ($n = 6$ cochleae). *Asterisks* indicate significant differences compared with the control data (*$p < 0.05$, **$p < 0.01$, ***$p < 0.0001$, Tukey–Kramer after one-way ANOVA). *n.s.*, not significant. Notably, because gluconate (129 mM) added to the low Cl⁻ solution affected the K⁺ exchanger in the microelectrode to some extent, the measurement of [K⁺] was relatively qualitative (see Supplemental Fig. 2)

difference across the marginal cell layer. Similar results were also observed in all five other cochleae; the [K⁺] and potential in the syncytial layer were 101.4 ± 8.2 mM and $+7.9 \pm 4.0$ mV, respectively, and the EP was $+83.1 \pm 4.4$ mV (mean ± SD, $n = 6$ cochleae, including the case shown in Fig. 1c). These observations agree with previous reports [1, 14, 26, 41] and thereby validate the experimental techniques used in the present study.

To characterize the elements that establish the positive RMP of fibrocytes, we perfused the scala tympani, a perilymphatic space, with solutions containing different Na⁺, K⁺, or Cl⁻ concentrations, while measuring the electrochemical properties of the lateral wall (Fig. 2). In each perfusate, we modified the concentration of individual ions without changing the total ion concentration. For this purpose, we used a solution containing cation concentrations of 100 mM Na⁺, 5 mM K⁺, and 46 mM NMDG as the control artificial perilymph (as previously outlined in the "Methods" section), the perfusion of which negligibly altered the EP (Supplemental Fig. 1). For some experiments, we intended to transiently insert a double-barreled K⁺-selective microelectrode across the syncytial layer, as shown in Fig. 1c, when the effects of the perfusates were stable. However, we could not determine the appropriate timing for microelectrode insertion. To resolve this problem, we placed a single-barreled microelectrode in the endolymph and monitored the EP throughout each experiment; this potential, which represents the transepithelial voltages across the lateral wall composed of the syncytial and marginal cell layers, is related to the membrane potential of fibrocytes (v_{FC}) according to the following Eq. [26, 27]:

$$EP = v_{FC} - v_{IM} + v_{MB} - v_{MA} \qquad (1)$$

where v_{IM}, v_{MB}, and v_{MA} correspond to the membrane potentials of intermediate cells, and basolateral and apical surfaces of marginal cells, respectively (see Fig. 1b). Each membrane potential was relative to the neighboring extracellular fluid, which was defined as 0 mV (see "Methods").

We first examined the effects of modulating [Na⁺] in the perilymph ([Na⁺]$_{PL}$) (Fig. 2A). As seen in Fig. 2Aa, the EP was relatively stable at approximately +85 mV during the application of the control solution. The K⁺-selective microelectrode was advanced across the lateral wall. Initially, the electrode in the perilymph recorded a [K⁺] of 5.2 mM (Fig. 2Ab). After further insertion, but before reaching the IS, we detected the syncytial layer composed of multiple fibrocytes ([K⁺], 57.6 to 99.7 mM; potential, +5.5 to +10.8 mV), as observed in the cochlea under physiological conditions (Fig. 1c). Within this region, peaks of relatively low [K⁺] (57.6 to 67.4 mM) can likely be attributed to processes in which the electrode penetrated the thin and infolded processes of the fibrocytes, or was transiently passed through the small quantity of cytoplasm. The compartment just prior to the IS showed the highest [K⁺] of 99.7 mM and the highest potential of +10.8 mV, which were defined as the properties of the syncytial layer. In the IS, the electrode recorded a low [K⁺] of 10.4 mM and

a

b
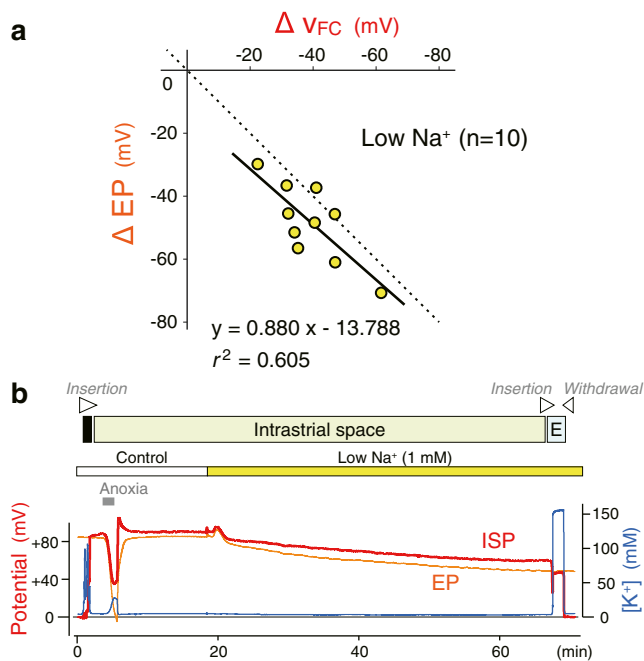
Fig. 4 Process of EP reduction during the perilymphatic perfusion of a low Na$^+$ solution. **a** Relationship between the reduction in the EP and the hyperpolarization of fibrocyte membrane potential (v_{FC}) under low perilymphatic [Na$^+$] ([Na$^+$]$_{PL}$) conditions. Data were obtained from the series of experiments summarized in Fig. 3. The *solid line* represents a linear regression fitted to the data (slope = 0.880, $r^2 = 0.605$) and the *broken line* represents the $y = x$ equivalence. **b** Analysis of the intrastrial space (IS). The EP (*orange*) continued to be monitored using a microelectrode in the endolymph. During the perilymphatic perfusion of the control solution, the K$^+$-selective double-barreled electrode was advanced from the perilymph toward the endolymph. During recording, the *wedges at the top of the panel* indicate the period during which the K$^+$-selective electrode was driven forward or backward through the lateral wall. The *bar filled with black above the trace* points to the syncytial layer. Imposition of anoxia caused a decrease in the potential of the IS (*ISP*) and an increase in [K$^+$] of the IS, as reported previously [26]. The perfusate was switched to a solution containing a low [Na$^+$] of 1 mM, as described by the *bar above the trace*. The K$^+$-selective electrode was further inserted into the endolymph (*E*) and finally retracted to the perilymphatic space

a high potential of +56.4 mV. Next, the perfusate was replaced with a low [Na$^+$] solution containing 1 mM Na$^+$ (Fig. 2Aa). Over the course of a few minutes, EP transiently increased by ~7 mV and then rapidly decreased from peak levels by ~15 mV. The potential continued to decline gradually, reaching a minimum of +35.9 mV after 1 h of perfusion. Then, we inserted a different K$^+$-selective microelectrode into the lateral wall (Fig. 2Ac). The IS was still characterized by low [K$^+$] (for the behavior of the IS properties, see Fig. 4). We found that the compartment just prior to the IS, which represented the syncytial layer, was hyperpolarized at −23.6 mV (Fig. 2Ac). Upon replacement of the low Na$^+$ solution with the control solution, the EP was recovered and approached baseline values (Fig. 2Aa). A different K$^+$-selective electrode that was advanced across the lateral wall when the EP became nearly plateaued recorded the representative

syncytial properties of 116.1 mM [K$^+$] and a +11.8 mV potential (Fig. 2Ad). This [K$^+$] value exceeded the syncytial [K$^+$] value detected during the first insertion of the electrode (99.7 mM; see Fig. 2Ab), despite the similarity in observed potential between the two trials (+10.8 mV in the first insertion). Nevertheless, in a statistical analysis of the measurements of the six cochleae with the protocol used in Fig. 2A, the difference in the syncytial [K$^+$] between the first and third insertion was not significant (5.5 mM increase on average; $t = 0.87$, $p = 0.4254$, two-tailed paired t test). Taken together, the results illustrated in Fig. 2A indicate that the reduction in [Na$^+$]$_{PL}$ caused v_{FC} to significantly hyperpolarize.

We further tested the solution containing a high [K$^+$] of 30 mM (Fig. 2B). As shown in Fig. 2Ba, the perfusion of this solution elevated the EP by ~15 mV over the course of a few minutes. This transient elevation may be an artifact resulting from the change in solution, as a similar phenomenon was observed when the control perilymph was switched to a low Na$^+$ solution in the scala tympani (Fig. 2Aa). Thereafter, the EP gradually decreased and showed some fluctuations, reaching a minimum of +66 mV in ~20 min. After the high [K$^+$] perfusate was washed using the control solution, the EP only exhibited minimal recovery. Such flickering and irreversibility suggest that high K$^+$ conditions can damage some cell types involved in EP formation. Nevertheless, this perturbation was likely to have only a moderate effect on syncytial properties; when EP was reduced to +67.3 mV during the perfusion of the high K$^+$ solution (Fig. 2Ba), v_{FC} and [K$^+$] in the syncytial layer ([K$^+$]$_{SY}$) were +6.2 mV and 121.3 mM, respectively (Fig. 2Bc), which were similar to the values observed during the infusion of the control solution (Fig. 2Bb). In addition, we found that the perfusion of the solution containing a low [Cl$^-$] of 2.4 mM decreased both EP and v_{FC} (Supplemental Fig. 2).

Figure 3 summarizes the effects of the perilymphatic perfusion of four different solutions, i.e., control, low Na$^+$, high K$^+$, and low Cl$^-$ (Fig. 2 and Supplemental Fig. 2), on the EP and electrochemical properties of the syncytial layer in numerous cochleae ($n = 28$, 10, 7, and 5 cochleae, respectively); one-way ANOVA was used to compare the results obtained for these solutions ($p < 0.0001$ for EP, $p < 0.0001$ for v_{FC}, and $p < 0.0001$ for [K$^+$]$_{SY}$). In this analysis, syncytial properties were determined when the EP became relatively stable during the application of each perfusate. As compared to the perfusion of the control solution, the application of the high K$^+$ solution (30 mM [K$^+$]) elevated [K$^+$]$_{SY}$ by ~1.2-fold (98.9 ± 9.7 mM; versus 117.0 ± 10.5 mV; $p = 0.0038$, Tukey–Kramer) and was expected to increase perilymphatic [K$^+$] ([K$^+$]$_{PL}$) by ~6-fold. Under these conditions, if the membranes of the fibrocytes were governed by K$^+$ permeability, v_{FC} should be significantly depolarized. However, there was no statistical difference between the results for the control solution and the high K$^+$ solution (+9.0 ± 3.7 versus +10.4 ± 2.3 mV; $p = 0.942$, Tukey–Kramer). Therefore, K$^+$ permeability may

not dominate the fibrocyte membranes. In support of this, v_{FC} was never depolarized, even when $[K^+]_{SY}$ was dramatically reduced to ~15 mM by the perilymphatic perfusion of artificial perilymph containing the Na^+/K^+ ATPase blocker ouabain [1]. Such a prominent change in intracellular $[K^+]$ would substantially rise the membrane potential if it was determined primarily by K^+ permeability (for localization of the ATPase, see Fig. 1b). Furthermore, if the fibrocyte membranes harbored abundant Cl^- permeability, then the application of a low Cl^- solution should significantly depolarize v_{FC}. The opposite result was obtained in our experiments ($+9.0 \pm 3.7$ mV for the control versus -0.9 ± 3.4 mV for low Cl^-; $p = 0.006$, Tukey–Kramer). It is again noteworthy that v_{FC} was remarkably hyperpolarized during the perfusion of the low Na^+ solution (-31.1 ± 11.2 mV; $n = 10$ cochleae) compared with the control solution ($p < 0.0001$, Tukey–Kramer). These observations indicate the possibility that fibrocyte membranes exhibit Na^+ permeability that exceeds the K^+ and Cl^- permeabilities under physiological conditions. Therefore, Na^+ permeability may play a key role in the maintenance of the positive RMP of fibrocytes. However, the contribution of K^+ and Cl^- permeability to fibrocyte RMP cannot be ruled out by our experimental findings (see "Discussion"). $[K^+]_{SY}$ during the perfusion of the low Na^+ solution was moderately lower than $[K^+]_{SY}$ under control conditions (76.5 ± 11.4 versus 98.9 ± 9.7 mM; $p < 0.0001$, Tukey–Kramer). The decrease in $[K^+]_{SY}$ may depolarize the membrane via K^+ permeability, and this element could be involved in changes in v_{FC}.

It is also possible that the perfusion of a low Na^+ solution alters the intracellular pH and/or $[Ca^{2+}]$ by modulating ion fluxes via Na^+ transporters expressed in fibrocytes, and this could hyperpolarize v_{FC} by affecting membrane permeability. Indeed, reverse transcription-PCR analysis detected mRNA of the Na^+/Ca^{2+} exchanger NCX1 in the lateral wall [29] and immunohistochemical assays detected protein of the Na^+/H^+ exchanger NHE1 in fibrocytes [2]. However, we found that the perilymphatic perfusion of benzamil (100 μM), an NCX1 inhibitor, had little effect on the EP that involves v_{FC} (Supplemental Fig. 3A) (Eq. 1). Furthermore, the application of amiloride (1 mM), which can block NHE1, to the scala tympani barely changed the EP in previous studies [10, 32]. This observation was also confirmed in our experiment (Supplemental Fig. 3B). Histochemical studies identified the expression of $Na^+/K^+/2Cl^-$ cotransporter type 1 (NKCC1) in fibrocytes [5, 25]. Perfusion of the low Na^+ solution to the scala tympani is expected to affect the function of NKCC. However, this process is unlikely to be associated with changes in v_{FC} because the transporter is electroneutral. In addition, we previously demonstrated that the perilymphatic perfusion of a NKCC blocker bumetanide minimally altered v_{FC} [41]. Taken together, it is probable that the hyperpolarization of v_{FC}

by the perfusion of a low Na^+ solution was not related to the effects on the aforementioned transporters, although effects of other unidentified Na^+-dependent carriers cannot be excluded.

Analysis of the reduction in EP caused by low $[Na^+]_{PL}$

We further examined the mechanism underlying the reduction in the EP via low $[Na^+]_{PL}$. Consistent with the results described in Fig. 2A, the steady-state value of the EP during the perfusion of a low Na^+ solution was significantly lower than that during the perfusion of the control solution, as shown in Fig. 3 ($+34.6 \pm 13.6$ versus $+80.7 \pm 5.8$ mV; $p < 0.0001$, Tukey–Kramer). The difference between these two average EP values (46.1 mM) resembled the difference between the average v_{FC} values between the two conditions (40.1 mM) (Fig. 3). This similarity led us to hypothesize that the EP loss is mainly attributable to the v_{FC} change (Eq. 1). In support of this, the hyperpolarized values of v_{FC} in the low Na^+ perfusion assays analyzed in Fig. 3 (10 cochleae) were highly correlated with the reduced values of EP (slope = 0.880, $r^2 = 0.605$) (Fig. 4a). To further confirm the above hypothesis, we analyzed other compartments of the lateral wall. We focused on the IS because the ISP stems from v_{FC} and v_{IM}, as described by the following Eq.:

$$ISP = v_{FC} - v_{IM} \tag{2}$$

Notably, the difference between the ISP and EP is equivalent to the transepithelial voltage across the marginal cell layer (see Fig. 1b):

$$EP = ISP + v_{MB} - v_{MA} \tag{3}$$

In the experiment shown in Fig. 4b, during the perfusion of the control solution into the scala tympani, the K^+-selective microelectrode held in the IS showed a potential of $+88.2$ mV and a $[K^+]$ of 5.1 mM. This ISP value was similar to the EP value ($+84.5$ mV) measured by a separate electrode in the endolymph. When the perfusate was replaced with a solution containing 1 mM $[Na^+]$, both ISP and EP decreased in a similar manner. This indicates that the transepithelial voltage across the marginal cell layer ($v_{MB} - v_{MA}$; see Eq. 3 and Fig. 1b) remained nearly unchanged and thereby contributed negligibly to EP loss (Eq. 1). In five experiments, including the example shown in Fig. 4b, the average maximum ISP reduction (36.0 ± 6.6 mV; steady state) was similar to the maximum EP reduction (40.6 ± 5.9 mV; steady state). These observations, in addition to the similarity between the v_{FC} hyperpolarization and the EP reduction (Fig. 4a), reinforce the idea that the v_{IM} alternation is limited and the EP change results primarily from the v_{FC} change (Eqs. 1–3). It is also noteworthy that the perfusion of a low Na^+ solution had little effect on $[K^+]_{IS}$ (Fig. 4b).
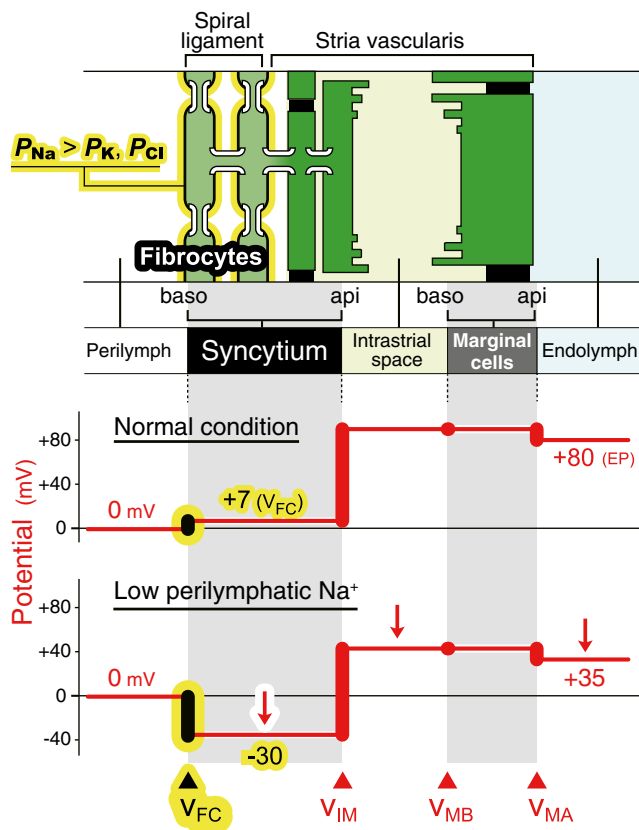
Fig. 5 A possible mechanism underlying the positive RMP in fibrocytes and its relevance to the EP. Our observations (Figs. 2, 3, and 4) imply that, in the fibrocyte membranes, Na^+ permeability (P_{Na}) exceeds the K^+ and Cl^- permeabilities (P_K and P_{Cl}, respectively), as shown in the *top panel*. This unique profile may continuously depolarize the membrane potential of the fibrocytes (v_{FC}) to ~+7 mV (from +5 to +12 mV) under physiological conditions (*middle panel*). When Na^+ was depleted in the perilymph (*bottom panel*), v_{FC} was remarkably hyperpolarized. In this situation, the EP was reduced as much as the v_{FC} is changed. v_{IM}, v_{MB}, and v_{MA} represent the membrane potential of intermediate cells, the basolateral surface of marginal cells, and the apical surface of marginal cells, respectively. The *top panel* was modified from Fig. 1 of our earlier work [26]

Discussion

Our electrophysiological experiments (Figs. 2 and 3) showed that v_{FC} was dramatically hyperpolarized by the perilymphatic application of a low Na^+ solution (Fig. 5) and this change was much larger than the changes induced by the perfusion of high K^+ or low Cl^- solutions. These results indicate that the membranes of cochlear fibrocytes likely exhibit Na^+ permeability and it significantly exceeds K^+ and Cl^- permeability (Fig. 5). Therefore, it is plausible that in these cells, Na^+ permeability plays key roles in the maintenance of the unusually positive RMP of +5 to +12 mV. The RMP is critical for harvesting the Kir4.1-induced K^+ diffusion potential on the intermediate-cell membranes to set the EP to a highly positive value, which is

essential for hearing (Figs. 1b and 5). This illustrates the crucial role of Na^+ permeability in the cochlea. In many excitable cell types, such as neurons and muscle cells, only slight Na^+ permeability is observed in the resting state, and it increases when an action potential is produced [4, 11, 15, 28]. Some non-excitable cell types, including renal epithelial cells, exhibit significant Na^+ permeability, but it is less than other ion permeabilities [30]. Accordingly, fibrocyte membrane profile appears to be relatively unique, although it may occur in other cell types that have not yet been characterized by electrophysiological experiments. The Na^+ equilibrium potential provided by measured $[Na^+]$ in the perilymph and the syncytial layer (146.6 and 33.9 mM, respectively [14]) is +39.1 mV. This value exceeds the recorded v_{FC} value (+5 to +12 mV) [1, 14,26, 41] (see also Fig. 2). This difference may be explained by permeability for other ion(s) than Na^+ and also electrogenicity of Na^+/K^+ ATPases.

The specific Na^+ conductance types involved in establishing the Na^+ permeability of fibrocytes remain unclear. Perilymphatic perfusion of tetrodotoxin, a voltage-gated Na^+ channel blocker, only slightly affected EP [21]. Nevertheless, the application of amiloride barely affected the EP [10, 32] (also see our experimental result in Supplemental Fig. 3B), suggesting little contribution from epithelial Na^+ channels (ENaCs) that form a constitutive active conductance. In support of this, the perfusion of benzamil at 100 µM, which also serves as a potent inhibitor of ENaCs (IC_{50}, 66 nM) [13], to the scala tympani negligibly suppressed the EP (Supplemental Fig. 3A). The proteins underlying fibrocyte Na^+ permeability should be identified in future studies.

Konishi and Kelsey (1968) and Shindo et al. (1992) reported that the perilymphatic perfusion of an Na^+-free solution had a minimal effect on the EP [21, 34]. Kuijpers and Bonting (1970) and Higashiyama et al. (2003) performed similar experiments and detected an EP reduction of ~15 mV [10, 24], but we observed more remarkable reductions in EP (~45 mV) (Figs. 2A and 3). Moreover, two groups have previously shown that the perfusion of a Cl^--free solution negligibly changes the EP [19, 34]. However, in our studies, a low Cl^- solution decreased the EP by ~40 mV (Fig. 3 and Supplemental Fig. 2). These inconsistencies may be related to differences in the efficiency of the perilymphatic perfusion. In previous studies [10, 21, 24, 34], the EP was only measured with a single-barreled glass microelectrode. Thus, the fenestra that was made on the bony wall of the cochlea for electrode insertion was likely small (for instance, ~50 µm in Kuijpers and Bonting [24]). We created a larger fenestra (200 × 500 µm; see "Methods") to simultaneously insert a double-barreled microelectrode and a single-barreled microelectrode (Figs. 2 and 4a and Supplemental Fig. 2). This fenestra, which was adjacent to the spiral ligament, may serve as a significant drainage pathway for solutions, in addition to the outlet hole made on the third turn, and thereby it could allow effective

perfusion across the fibrocytes. Notably, potential leakage of solutions through the fenestra was unlikely to affect the stability of electrophysiological measurements because the perfusion of control artificial perilymph minimally altered the EP values (Supplemental Fig. 1).

The mechanism underlying the reduction in the EP for a low Cl^- solution remains uncertain, but may involve outer sulcus cells and/or Reissner's membrane epithelial cells, both of which are exposed to the perilymph and express Cl^- channels or transporters [18, 31]. These cells constitute the boundary between perilymph and endolymph and they are believed to contribute to the EP. This hypothesis should be confirmed by electrophysiological assays.

Compliance with ethical standards

Conflict of interest None.

Ethical standards The experiments comply with the current laws of Japan.

References

1. Adachi N, Yoshida T, Nin F, Ogata G, Yamaguchi S, Suzuki T, Komune S, Hisa Y, Hibino H, Kurachi Y (2013) The mechanism underlying maintenance of the endocochlear potential by the K^+ transport system in fibrocytes of the inner ear. J Physiol 591:4459–72. doi:10.1113/jphysiol.2013.258046

2. Bond BR, Ng LL, Schulte BA (1998) Identification of mRNA transcripts and immunohistochemical localization of Na/H exchanger isoforms in gerbil inner ear. Hear Res 123:1–9. doi:10.1016/S0378-5955(98)00089-6

3. Chan DK, Hudspeth AJ (2005) Ca^{2+} current-driven nonlinear amplification by the mammalian cochlea in vitro. Nat Neurosci 8:149–55. doi:10.1038/nn1385

4. Coster J, Siegelbaum S (2013) Membrane potential and the passive electrical properties of the neuron. In: Kandel ER, Schartz JH, Jessel TM, Siegelbaum SA, Hudspeth AJ (eds) Principles of neural science. McGraw-Hill, NY

5. Crouch JJ, Sakaguchi N, Lytle C, Schulte BA (1997) Immunohistochemical localization of the Na-K-Cl co-transporter (NKCC1) in the gerbil inner ear. J Histochem Cytochem 45:773–8. doi:10.1177/002215549704500601

6. Davis H (1961) Some principles of sensory receptor action. Physiol Rev 41:391–416, PMID: 13720173

7. Gow A, Davies C, Southwood CM, Frolenkov G, Chrustowski M, Ng L, Yamauchi D, Marcus DC, Kachar B (2004) Deafness in Claudin 11-null mice reveals the critical contribution of basal cell tight junctions to stria vascularis function. J Neurosci 24:7051–62. doi:10.1523/JNEUROSCI.1640-04.2004

8. Hibino H, Inanobe A, Furutani K, Murakami S, Findlay I, Kurachi Y (2010) Inwardly rectifying potassium channels: their structure, function, and physiological roles. Physiol Rev 90:291–366. doi:10.1152/physrev.00021.2009

9. Hibino H, Kurachi Y (2006) Molecular and physiological bases of the K^+ circulation in the mammalian inner ear. Physiology (Bethesda) 21:336–45. doi:10.1152/physiol.00023.2006

10. Higashiyama K, Takeuchi S, Azuma H, Sawada S, Yamakawa K, Kakigi A, Takeda T (2003) Bumetanide-induced enlargement of the intercellular space in the stria vascularis critically depends on Na^+ transport. Hear Res 186:1–9. doi:10.1016/s0378-5955(03)00226-0

11. Hille B (2001) Ion channels of excitable membranes, 3rd edn. Sinauer, Sunderland, MA

12. Hinojosa R, Rodriguez-Echandia EL (1966) The fine structure of the stria vascularis of the cat inner ear. Am J Anat 118:631–63. doi:10.1002/aja.1001180218

13. Hirsh AJ, Molino BF, Zhang J, Astakhova N, Geiss WB, Sargent BJ, Swenson BD, Usyatinsky A, Wyle MJ, Boucher RC, Smith RT, Zamurs A, Johnson MR (2006) Design, synthesis, and structure-activity relationships of novel 2-substituted pyrazinoylguanidine epithelial sodium channel blockers: drugs for cystic fibrosis and chronic bronchitis. J Med Chem 49:4098–115. doi:10.1021/jm051134w

14. Ikeda K, Morizono T (1989) Electrochemical profiles for monovalent ions in the stria vascularis: cellular model of ion transport mechanisms. Hear Res 39:279–86. doi:10.1016/0378-5955(89)90047-6

15. Jaye DA, Xiao Y-F, Sigg DC (2010) Basic cardiac electrophysiology: Excitable membranes. In: Sigg CD, Iaizzo AP, Xiao Y-F, He B (eds) Cardiac electrophysiology methods and models. Springer US, Boston, MA, pp 41–51. doi:10.1007/978-1-4419-6658-2_2

16. Kelly JJ, Forge A, Jagger DJ (2012) Contractility in type III cochlear fibrocytes is dependent on non-muscle myosin II and intercellular gap junctional coupling. J Assoc Res Otolaryngol 13:473–84. doi:10.1007/s10162-012-0322-7

17. Kikuchi T, Kimura RS, Paul DL, Adams JC (1995) Gap junctions in the rat cochlea: immunohistochemical and ultrastructural analysis. Anat Embryol (Berl) 191:101–18. doi:10.1007/BF00186783

18. Kim KX, Sanneman JD, Kim HM, Harbidge DG, Xu J, Soleimani M, Wangemann P, Marcus DC (2014) Slc26a7 chloride channel activity and localization in mouse Reissner's membrane epithelium. PLoS One 9, e97191. doi:10.1371/journal.pone.0097191

19. Kitano I, Doi K, Mori N, Matsunaga T (1993) Involvement of Cl^- transport in forskolin-induced elevation of endocochlear potential. Hear Res 71:23–7. doi:10.1016/0378-5955(93)90017-U

20. Kohl P, Gourdie RG (2014) Fibroblast–myocyte electrotonic coupling: does it occur in native cardiac tissue? J Mol Cell Cardiol 70:37–46. doi:10.1016/j.yjmcc.2013.12.024

21. Konishi T, Kelsey E (1968) Effect of sodium deficiency on cochlear potentials. J Acoust Soc Am 43:462–70. doi:10.1121/1.1910853

22. Konishi T, Salt AN (1983) Electrochemical profile for potassium ions across the cochlear hair cell membranes of normal and noise-exposed guinea pigs. Hear Res 11:219–33. doi:10.1016/0378-5955(83)90080-1

23. Kuijpers W, Bonting SL (1970) The cochlear potentials. I. The effect of ouabain on the cochlear potentials of the guinea pig. Pflugers Arch 320:348–58. doi:10.1007/BF00588213

24. Kuijpers W, Bonting SL (1970) The cochlear potentials. II. The nature of the cochlear endolymphatic resting potential. Pflugers Arch 320:359–72. doi:10.1007/BF00588214

25. Mizuta K, Adachi M, Iwasa KH (1997) Ultrastructural localization of the Na-K-Cl cotransporter in the lateral wall of the rabbit cochlear duct. Hear Res 106:154–62. doi:10.1016/S0378-5955(97)00010-5

26. Nin F, Hibino H, Doi K, Suzuki T, Hisa Y, Kurachi Y (2008) The endocochlear potential depends on two K$^+$ diffusion potentials and an electrical barrier in the stria vascularis of the inner ear. Proc Natl Acad Sci U S A 105:1751–6. doi:10.1073/pnas.0711463105

27. Nin F, Hibino H, Murakami S, Suzuki T, Hisa Y, Kurachi Y (2012) Computational model of a circulation current that controls electrochemical properties in the mammalian cochlea. Proc Natl Acad Sci U S A 109:9191–6. doi:10.1073/pnas.1120067109

28. Noble D (1984) The surprising heart: a review of recent progress in cardiac electrophysiology. J Physiol 353:1–50. doi:10.1113/jphysiol.1984.sp015320

29. Oshima T, Ikeda K, Furukawa M, Takasaka T (1997) Alternatively spliced isoforms of the Na$^+$/Ca^{2+} exchanger in the guinea pig cochlea. Biochem Biophys Res Commun 233:737–41. doi:10.1006/bbrc.1997.6533

30. Rodan AR, Cheng CJ, Huang CL (2011) Recent advances in distal tubular potassium handling. Am J Physiol Renal Physiol 300:F821–7. doi:10.1152/ajprenal.00742.2010

31. Royaux IE, Belyantseva IA, Wu T, Kachar B, Everett LA, Marcus DC, Green ED (2003) Localization and functional studies of pendrin in the mouse inner ear provide insight about the etiology of deafness in pendred syndrome. JARO 4:394–404. doi:10.1007/s10162-002-3052-4

32. Salt A, Konishi T (1979) The role of potassium and sodium in cochlear transduction: a study with amiloride and tetraethylammonium. J Acoust Soc Am 66:S47. doi:10.1121/1.2017784

33. Salt AN, Melichar I, Thalmann R (1987) Mechanisms of endocochlear potential generation by stria vascularis. Laryngoscope 97:984–91. doi:10.1288/00005537-198708000-00020

34. Shindo M, Miyamoto M, Abe N, Shida S, Murakami Y, Imai Y (1992) Dependence of endocochlear potential on basolateral Na$^+$ and Cl$^-$ concentration: a study using vascular and perilymph perfusion. Jpn J Physiol 42:617–30. doi:10.2170/jjphysiol.42.617

35. Spicer SS, Schulte BA (1996) The fine structure of spiral ligament cells relates to ion return to the stria and varies with place-frequency. Hear Res 100:80–100. doi:10.1016/0378-5955(96)00106-2

36. Takahashi T, Kimura RS (1970) The ultrastructure of the spiral ligament in the Rhesus monkey. Acta Otolaryngol 69:46–60. doi:10.3109/00016487009123335

37. Takeuchi S, Ando M (1998) Dye-coupling of melanocytes with endothelial cells and pericytes in the cochlea of gerbils. Cell Tissue Res 293:271–5. doi:10.1007/s004410051118

38. Takeuchi S, Ando M, Kakigi A (2000) Mechanism generating endocochlear potential: role played by intermediate cells in stria vascularis. Biophys J 79:2572–82. doi:10.1016/S0006-3495(00)76497-6

39. Wangemann P (2006) Supporting sensory transduction: cochlear fluid homeostasis and the endocochlear potential. J Physiol 576:11–21. doi:10.1113/jphysiol.2006.112888

40. Weber PC, Cunningham CD 3rd, Schulte BA (2001) Potassium recycling pathways in the human cochlea. Laryngoscope 111:1156–65. doi:10.1097/00005537-200107000-00006

41. Yoshida T, Nin F, Ogata G, Uetsuka S, Kitahara T, Inohara H, Akazawa K, Komune S, Kurachi Y, Hibino H (2015) NKCCs in the fibrocytes of the spiral ligament are silent on the unidirectional K$^+$ transport that controls the electrochemical properties in the mammalian cochlea. Pflugers Arch 467:1577–89. doi:10.1007/s00424-014-1597-9

42. Zdebik AA, Wangemann P, Jentsch TJ (2009) Potassium ion movement in the inner ear: insights from genetic disease and mouse models. Physiology (Bethesda) 24:307–16. doi:10.1152/physiol.00018.2009

43. Zuidema T, Dekker K, Vanheukelom JS (1985) The influence of organic counterions on junction potentials and measured membrane potentials. Bioelectrochem Bioenerg 14:479–94. doi:10.1016/0302-4598(85)80020-9